SLAC NATIONAL ACCELERATOR LABORATORY

SuperCDMS SNOLAB Low-Mass Dark Matter Detectors

Noah Kurinsky, *Paul Brink, Richard Partridge, Blas Cabrera, Matt Pyle*
on behalf of the SuperCDMS Collaboration

SLAC National Accelerator Laboratory & Stanford University
Kavli Institute for Particle Astrophysics and Cosmology
Menlo Park, CA 94025, USA

ICHEP2016CHICAGO

Detector Simulation

Our ability to measure the energy of events depends critically on our detailed knowledge of the electric field within our detectors. As the electrons and holes are accelerated through the electric field, they emit Luke-Neganov phonons to maintain constant drift speed, resulting in additional phonon energy proportional to voltage across the crystal:

$$E_{phonon} = \left(\frac{y(E_{recoil}) * (V - \varepsilon_{bandgap})}{\varepsilon_{eh}} + 1\right) E_{recoil}$$

The energy depends on the bandgap and energy per electron-hole pair and charge yield, but primarily on the potential different crossed when that potential is much greater than either of the other energy scales.

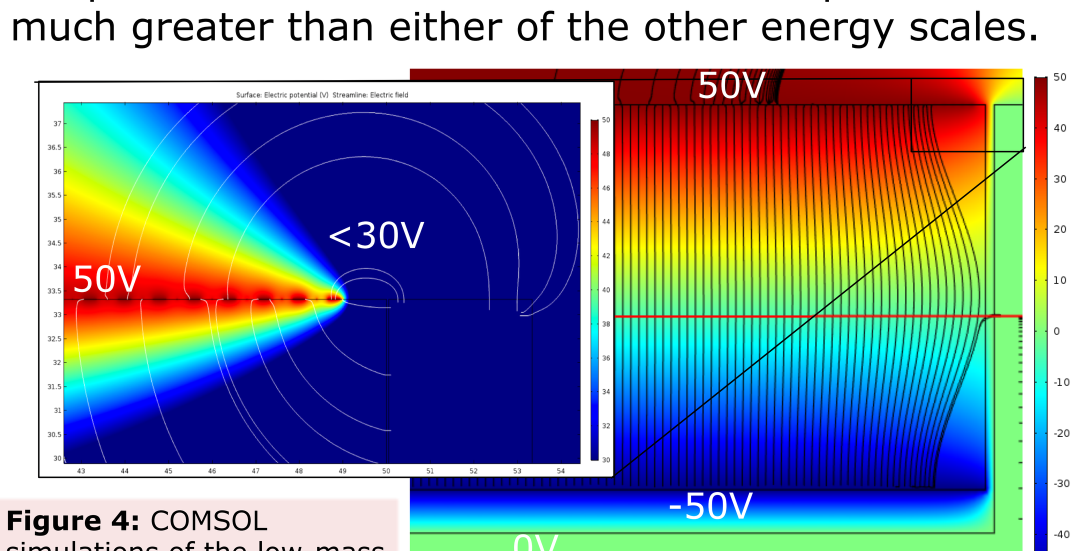

Figure 4: COMSOL simulations of the low-mass detector electric fields

Figure courtesy Angela Bai

We need to reject events that experience a non-uniform field. We employ COMSOL to simulate detailed field in our crystal, including the effect on the field/potential due to the grounded detector housing (above right) and surface field and potential fluctuations between wires and sensors (left). We use these fields and our detector Monte-Carlo to determine where the full-scale potential yield drops at the edge of the crystal (below).

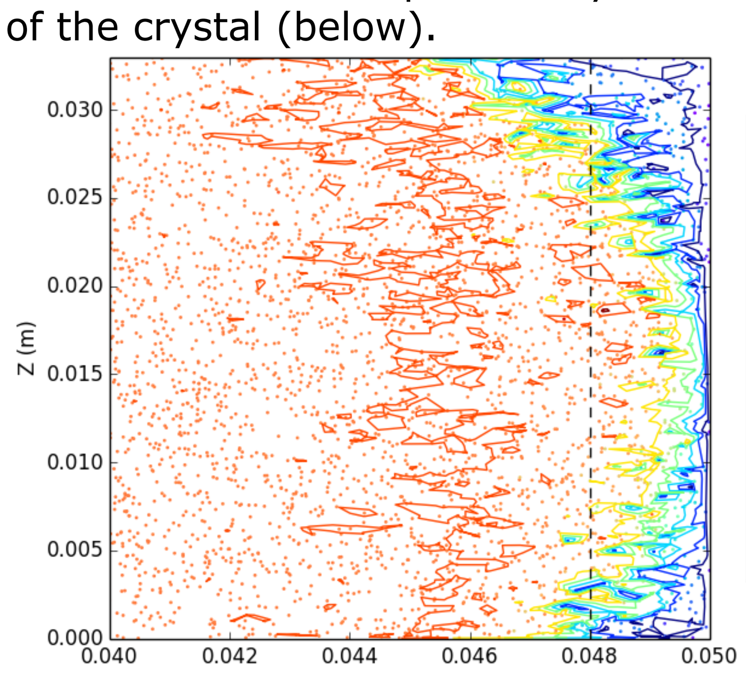

Figure 5: Energy yield (Output/Input Energy) produced by an event at the indicated point divided by input energy, with detector efficiencies and gain taken into account. Inside 45mm, the gain is constant.

Position Reconstruction

The sensor layout in our detectors was chosen based on a study of 8 potential layouts, compared using the detector Monte Carlo for energy resolution and surface event rejection. We want to reject low-yield events and all events from backgrounds which largely present at the detector surfaces.

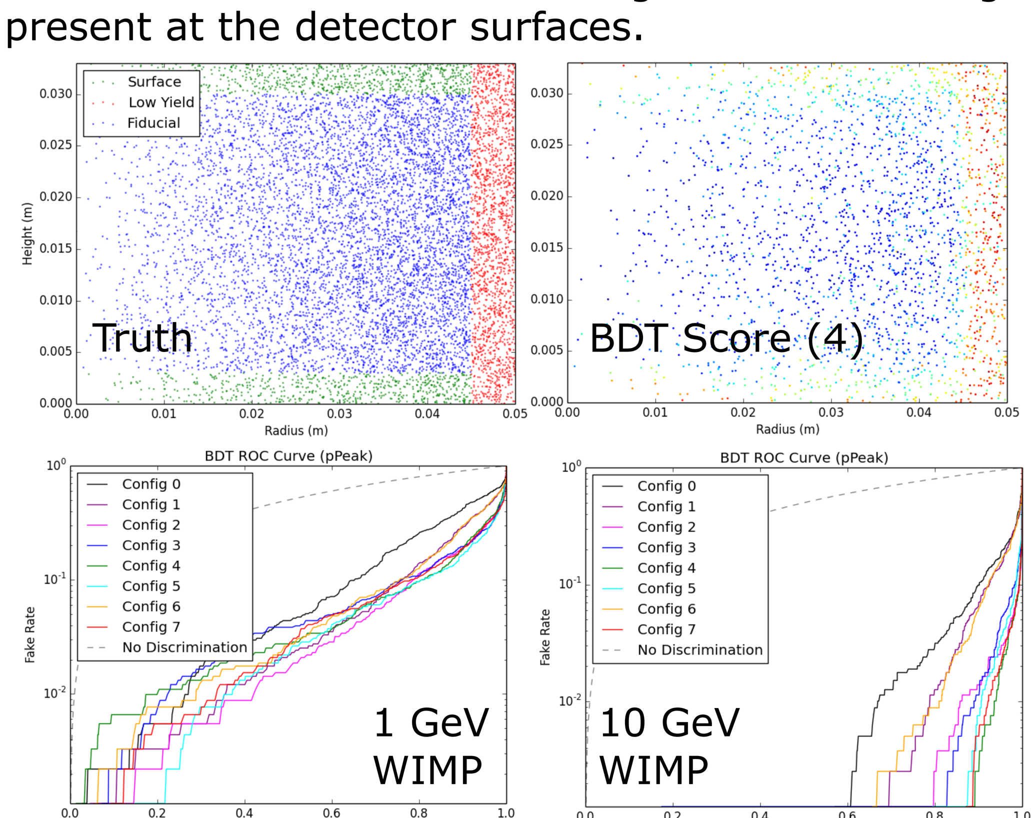

Figure 6: These plots demonstrate rejection ability for different energy regimes. A boosted decision tree was trained to identify bulk/surface events from a range of position-dependent quantities. The 10 GeV regime contains more strong lines, and is more crucial to be able to fiducialize; the 1 GeV regime is more intrinsically quiet as there are no strong decay lines in the energy regime of interest, so the weaker rejection power is less important.

Abstract

We present the proposed design for the SuperCDMS high-voltage, low-mass dark matter detectors, designed to be sensitive to dark matter down to 300 MeV in mass and resolve individual electron-hole pairs from low-energy scattering events in high-purity Ge and Si crystals. In this note we discuss the studies and technological improvements which have allowed us to design such a sensitive detector, including advances in phonon sensor design and detector simulation.

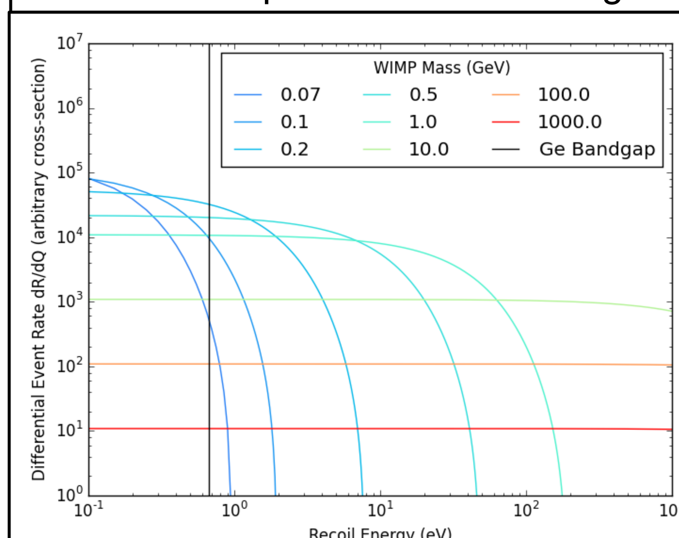

Figure 1: Differential event rate for various WIMP masses in Ge, based on an arbitrary wimp-nucleon scattering cross-section. Low energy behavior is determined by density (decreases with mass), high energy by Maxwellian velocity distribution (increases with mass). Ge/Si bandgaps set minimum WIMP mass observable by our semiconductor detectors

To probe light dark matter, we need to lower energy thresholds by

- **Achieving better than 10eV in phonon resolution**, an order of magnitude improvement over past devices (below)
- Employing Luke-Neganov gain to **convert the charge signal into a boosted phonon signal** (upper left)
- **Improving our event reconstruction** to reject additional sources of noise (lower left)

Phonon Sensor Design

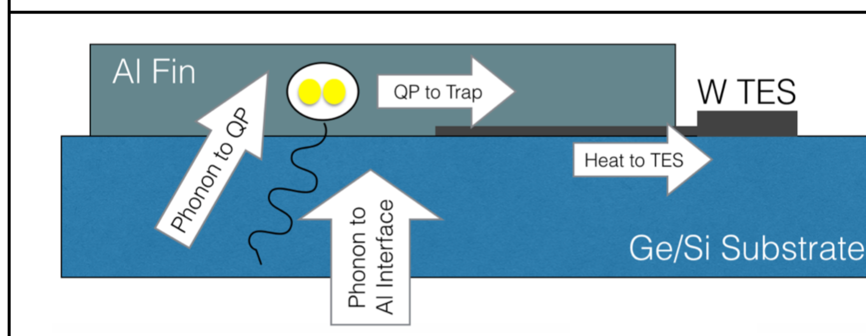

Figure 2: 2D slice of a phonon sensor, showing the energy transport steps. Each arrow carries an associated efficiency; the phonon to QP process is fundamentally ~60% efficient for example.

Phonons are collected in superconducting aluminum fins, breaking cooper-pairs, and the resulting quasiparticles are trapped on tungsten spurs which channel energy to the TES. Much of the optimization lies in relative sizing of aluminum fins and tungsten traps.

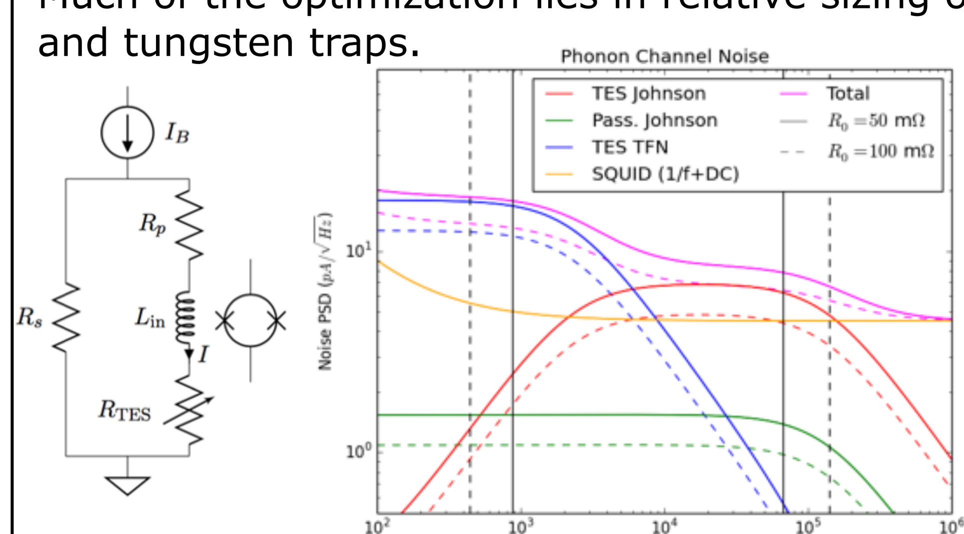

Figure 3: (Left) TES voltage-bias circuit showing elements which contribute to noise budget. (right) expected noise contribution from circuit elements. Signal lies between vertical lines. Elements designed to be subdominant to TES in signal region. TES has fixed normal resistance based on noise considerations

The current in the TES is read out by a SQUID, and the heat capacity of the TES along with the squid inductance creates an LRC-like response. We tune the resistance of the TES to produce an over-damped response, as the current response fall-time sets the energy resolution of the sensor.

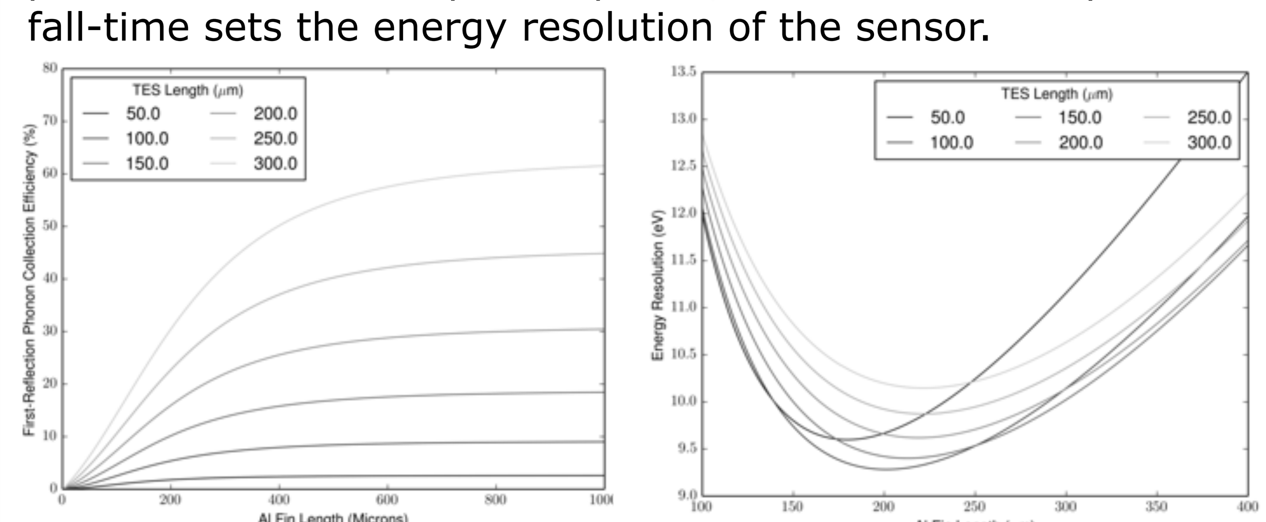

Longer TES allows for more phonon sensors (TES wired in parallel) and quicker phonon absorption (shorter pulses, lower resolution). Longer fins have lower collection efficiency but faster pulses. Left shows position sensitivity, right resolution.

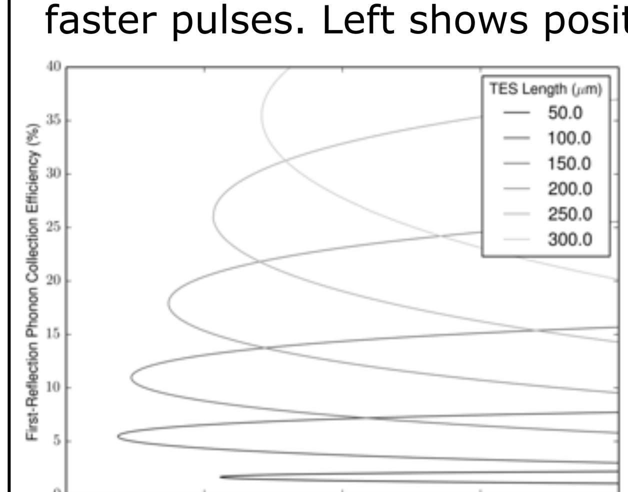

Left plot shows simultaneous optimization; we choose longest TES that will meet energy resolution goal (200 microns), and make fins slightly longer to gain more position sensitivity (fins chosen to be 240 microns long). Energy resolution assumes all channels used (worst case scenario)

Detector Layout

Each face of the detector is instrumented with 6 channels of TES sensors wired in parallel, with wires running to radial contacts. Wires are super-conducting aluminum

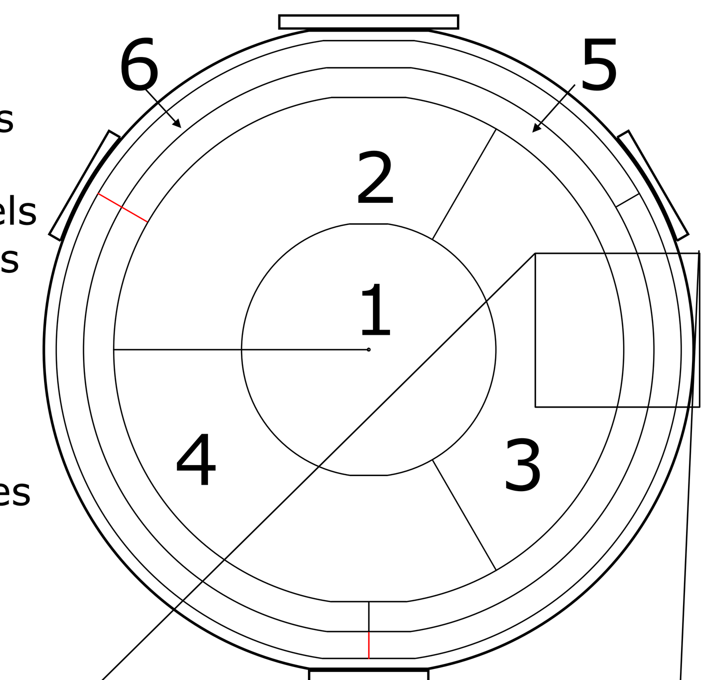

Phonon sensors arranged in a grid for maximum field/phonon absorption uniformity. Outer grid helps to improve field uniformity.

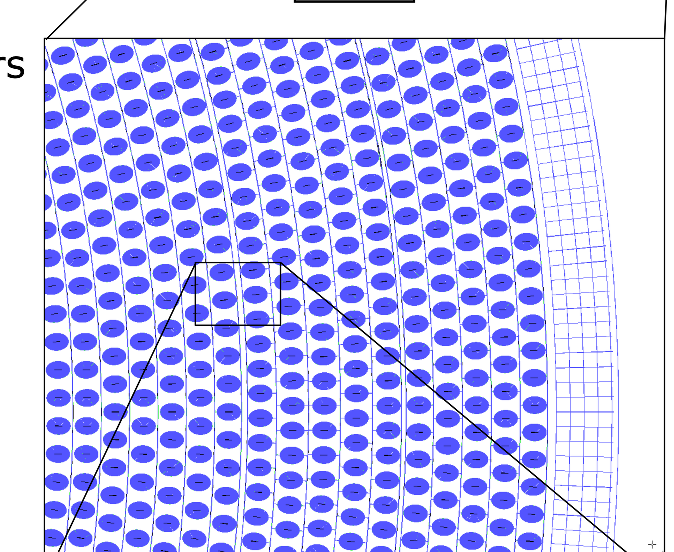

Sensors share common bias rails to decrease non-instrumented aluminum, which acts as a phonon sink.

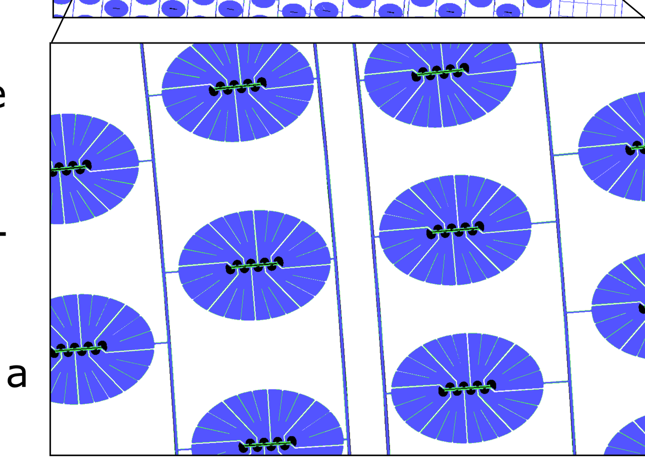

Each sensor consists of aluminum fins surrounding a central tungsten TES. The fins are coupled to the TES through the semicircular overlap regions. We place slots in the fins to allow for multiple TES connections and make diffusion more 1D. Smaller slots prevent magnetic flux trapping.

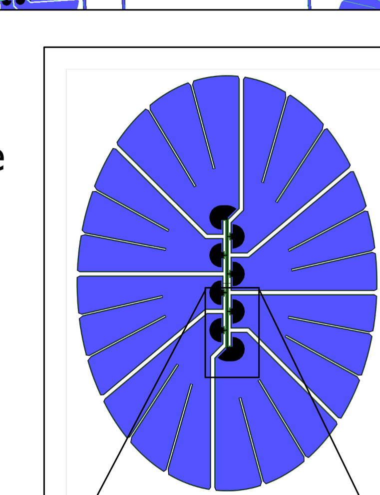

The overlap regions are designed to maximize quasiparticle collection efficiency and minimize resulting qp diffusion length after trapping into the TES. The tungsten (black) underneath the fins is proximitized by the aluminum, and does not contribute to the TES noise budget, but the smaller connectors do.

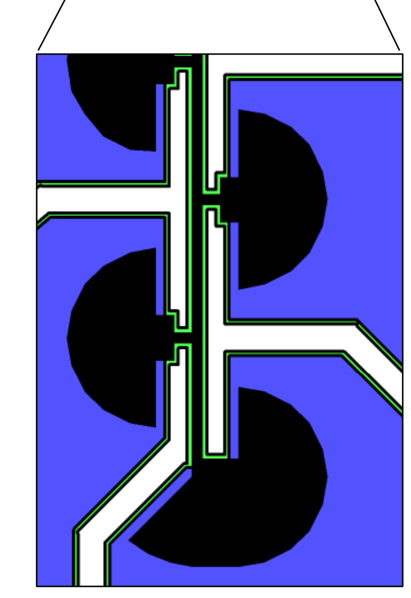

The green is a dielectric layer used to prevent leakage current across the detector, which is a major concern in a 3 cm thick detector which needs to hold up to 100V of potential bias between faces.

References

J. J. Yen, et. al., "Measurement Of Quasiparticle Transport In Al Films Using Tungsten Transition-Edge Sensors", App. Phys. Lett. 105, 163504 (2014).

R. Agnese *et al.* (SuperCDMS collaboration), "Search for Low-Mass Weakly Interacting Massive Particles Using Voltage-Assisted Calorimetric Ionization Detection in the SuperCDMS Experiment" (CDMSlite), Phys. Rev. Lett. **112**, 041302

V S Vavilov. "Radiation ionization processes in germanium and silicon crystals". Soviet Physics Uspekhi, 4(5):761, 1962

K.D. Irwin and G.C. Hilton. "Transition-edge sensors". In Christian Enss, editor, Cryogenic Particle Detection, volume 99 of Topics in Applied Physics, pages 63{150. Springer Berlin Heidelberg, 2005